

CP violation in the Standard Model with a complex singlet

Neda Darvishi* and Maria Krawczyk†
*Faculty of Physics, University of Warsaw,
Pasteura 5, 02-093 Warsaw, Poland*

CP violation of the Standard Model (SM) is insufficient to explain the baryon asymmetry in the Universe and therefore an additional source of CP violation is needed. Here we consider the extension of the SM by a neutral complex singlet and discuss the physical conditions for a spontaneous CP violation in such model. In the model there are three neutral Higgs particles. Assuming the lightest one to be the 125 GeV Higgs boson found at LHC we calculate masses of the additional Higgs scalars and perform a numerical study of the allowed region of parameters. The scenario according to which the SM-like Higgs particle comes mostly from the SM-like SU(2) doublet, with a small modification coming from the singlet, is in agreement with the newest $R_{\gamma\gamma}$ and precise EW (parameters S, T) data. We have found that the Jarlskog invariant, measuring the strength of the CP violation, can be enhanced as compared to the one in the SM, at the same time there is no corresponding enhancements expected for the Electric Dipole Moment (EDM).

I. INTRODUCTION

It is well known that in the Standard Model (SM), where CP is explicitly broken at the Lagrangian level through the complex Yukawa couplings, the single phase in the Cabibbo-Kobayashi-Maskawa matrix (CKM) is a unique source of CP violation. According to Sakharov [1], there are three requirements that must be satisfied in order to generate the baryon asymmetry of the Universe, namely the violation of the baryon number, violation of C and CP symmetries and the existence of non equilibrium processes, see also reference [2]. In spite of satisfying these demands, the amount of CP violation within the SM is not sufficient to explain the observed baryon asymmetry of the Universe [3–5]. In order to have an extra source of CP violation, that could allow to address this important issue, various extensions of the SM are considered [6–11].

Here we shall assume that the additional sources of CP violation are provided by a neutral complex scalar singlet χ , which accompanies the SM-like Higgs doublet Φ . This kind of extension of the SM was discussed in the literature with various motivations, see e.g. [12–21]. We consider the potential with a softly broken global U(1) symmetry, which we call the Constrained SM+CS model (cSMCS). Assuming nonzero vacuum expectation value for the complex singlet we analyse the physical conditions for spontaneously CP violation. In the model there are three neutral Higgs particles with mixed CP properties. Assuming the lightest one, predominately CP-even, to be 125 GeV Higgs boson found at LHC, we calculate masses of the other Higgs scalars and perform a numerical study of the allowed region of parameters. We calculate the Jarlskog invariant [22–25], measuring the amount of the CP violation in our model, and comment the prediction of the model for the electric dipole moment EDM. The

scenario realized in the model according to which the SM-like Higgs particle comes mostly from the SM-like SU(2) doublet with a small modification coming from the singlet, is in agreement with the newest LHC Higgs data, in particular the strength signal $R_{\gamma\gamma}$, as well as the precise EW measurements. We propose the benchmarks to test this model.

The model considered in this paper is a part of a larger framework introduced in [26, 27], where the extension of the SM by a complex singlet and the inert doublet (with $vev = 0$) has been studied, with the focus on the properties of dark matter. Here we focus on the issue of a CP violation due to a complex singlet with a complex expectation value. This model offers a possibility of the strong first-order phase-transition, and if extended by vector quarks leads to a proper description of baryogenesis, what is shown in [28].

The content of this paper is as follows. In section II a general presentation of the SMCS model and its constrained version (cSMCS) investigated in the paper is given. In particular, the subsection II C describes the conditions for the spontaneous CP violation in the model. Physical states in the Higgs sector are discussed in section IX B. The numerical results of scans over parameters of the model are collected in sec. IV. In the section V the Jarlskog invariant for the scalars is discussed. In the section VI the agreement of cSMCS model with existing LHC measurements of the properties of the SM-like Higgs boson as well as comparison with data on S and T parameters are shown. Here also we comment on predictions of the model on the EDM. The benchmarks are presented here as well. Section VII contains the conclusion. Detailed formulas are presented in the Appendix.

II. THE CSMCS: THE SM PLUS A COMPLEX SINGLET

The full Lagrangian of the model is given by

$$\mathcal{L} = \mathcal{L}_{gf}^{SM} + \mathcal{L}_{scalar} + \mathcal{L}_Y(\psi_f, \Phi), \quad \mathcal{L}_{scalar} = T - V, \quad (1)$$

* neda.darvishi@fuw.edu.pl

† maria.krawczyk@fuw.edu.pl

where \mathcal{L}_{gf}^{SM} describes the pure gauge bosons terms as well the SM boson-fermion interaction, \mathcal{L}_{scalar} describes the scalar sector of the model with one SU(2) doublet Φ and a neutral complex scalar (spinless) singlet χ . $\mathcal{L}_Y(\psi_f, \Phi)$ represents the Yukawa interaction of Φ with the SM fermions. The neutral complex scalar singlet χ does not couple to the SM fermions and therefore the singlet-fermion interaction is present only through the mixing of the singlet χ with the doublet Φ , the same holds for singlet interaction with the gauge bosons. This model allows for the SM-like scenario observed at the LHC, with the SM-like Higgs boson predominantly consisting of a neutral CP-even component of the Φ doublet.

We assume Φ and χ fields have vacuum expectation values (vev) v and $we^{i\xi}$, respectively, where $v, w, \xi \in \mathbf{R}$. We shall use the following field decomposition around the vacuum state:

$$\Phi = \begin{pmatrix} \phi^+ \\ \frac{1}{\sqrt{2}}(v + \phi_1 + i\phi_4) \end{pmatrix}, \chi = \frac{1}{\sqrt{2}}(we^{i\xi} + \phi_2 + i\phi_3). \quad (2)$$

Masses of the EW gauge bosons and the fermions are given by the vev of the doublet, e.g. $M_W^2 = g^2 v^2/4$ for the W boson.

A. Potential

The scalar potential of the model can be written as follows

$$V = V_D + V_S + V_{DS}, \quad (3)$$

with the pure doublet and the pure singlet parts (respectively V_D and V_S) and their interaction term V_{DS} . The SM part of the potential, V_D , is given by:

$$V_D = -\frac{1}{2}m_{11}^2 \Phi^\dagger \Phi + \frac{1}{2}\lambda_1 (\Phi^\dagger \Phi)^2. \quad (4)$$

The potential for a complex singlet is equal to:

$$\begin{aligned} V_S = & -\frac{1}{2}m_s^2 \chi^* \chi - \frac{1}{2}m_4^2 (\chi^{*2} + \chi^2) \\ & + \lambda_{s1} (\chi^* \chi)^2 + \lambda_{s2} (\chi^* \chi) (\chi^{*2} + \chi^2) + \lambda_{s3} (\chi^4 + \chi^{*4}) \\ & + \kappa_1 (\chi + \chi^*) + \kappa_2 (\chi^3 + \chi^{*3}) + \kappa_3 (\chi^* \chi) (\chi + \chi^*). \end{aligned} \quad (5)$$

The doublet-singlet interaction terms are:

$$\begin{aligned} V_{DS} = & \Lambda_1 (\Phi^\dagger \Phi) (\chi^* \chi) + \Lambda_2 (\Phi^\dagger \Phi) (\chi^{*2} + \chi^2) \\ & + \kappa_4 (\Phi^\dagger \Phi) (\chi + \chi^*). \end{aligned} \quad (6)$$

There are three quadratic (m_a^2), six dimensionless quartic (λ_a, Λ_a) and four dimensionful parameters κ_i , $i = 1, 2, 3, 4$, describing linear (κ_1), cubic (κ_2, κ_3) and mixed (κ_4) terms, respectively. The linear term κ_1 can be removed by a translation of the singlet field, and therefore can be neglected.

To simplify the model, we apply a global U(1) symmetry

$$U(1) : \Phi \rightarrow \Phi, \chi \rightarrow e^{i\alpha} \chi \quad (7)$$

to reduce the number of parameters in the potential [26]. However, a non-zero vev of χ would lead in such case to a spontaneous breaking of this symmetry and an appearance of massless Nambu-Goldstone scalar particles, what is not acceptable. Keeping some U(1) soft-breaking terms in the potential would solve this problem and at the same time would still lead to a reduction of the number of parameters of V . In what follows, we shall consider a potential with a soft-breaking of U(1) symmetry, where the singlet cubic terms $\kappa_{2,3}$ and the singlet quadratic term m_4^2 are kept. For simplicity the κ_4 term is neglected in the main part of analysis, see also discussion in [26]. We assume it is negligible, being generated at one loop with strength given by $\frac{1}{16\pi^2} \kappa_3 \Lambda_1$ [29], where coupling Λ we keep small to ensure perturbativity of our calculation. We have checked that neglecting the κ_4 term does not change basic properties of the model. Some results for the case with non-zero κ_4 are presented in the Appendix IX.

In the analysis of the model we include the U(1)-symmetric terms ($m_{11}^2, m_s^2, \lambda_1, \lambda_{s1}, \Lambda_1$) and the U(1)-soft-breaking terms ($m_4^2, \kappa_{2,3}$). Simplifying slightly the notation by using: $\lambda_s = \lambda_{s1}, \Lambda = \Lambda_1$, we get the potential in the following form

$$\begin{aligned} V = & -\frac{1}{2}m_{11}^2 \Phi^\dagger \Phi + \frac{1}{2}\lambda_1 (\Phi^\dagger \Phi)^2 \\ & -\frac{1}{2}m_s^2 \chi^* \chi + \lambda_s (\chi^* \chi)^2 + \Lambda (\Phi^\dagger \Phi) (\chi^* \chi) \\ & -\frac{1}{2}m_4^2 (\chi^{*2} + \chi^2) + \kappa_2 (\chi^3 + \chi^{*3}) + \kappa_3 (\chi^* \chi) (\chi + \chi^*). \end{aligned} \quad (8)$$

With all parameter real the potential V is explicitly symmetric under the CP transformation $\Phi \rightarrow \Phi^\dagger, \chi \rightarrow \chi^*$. We shall call the model with this choice of parameters, cSMCS [27].

Note, that this potential (65) is similar to the potential with two real singlets, with an additional Z_2 symmetry for the one singlet field, considered in paper [20]. In that model, however, CP violation is not possible.

Useful form of potential is obtained if the complex scalar χ is expressed in terms of its real and imaginary parts, $\chi = (\chi_1 + i\chi_2)/\sqrt{2}$, namely

$$\begin{aligned} V = & -\frac{1}{2}m_{11}^2 \Phi^\dagger \Phi + \frac{1}{2}\lambda_1 (\Phi^\dagger \Phi)^2 \\ & -\frac{\mu_1^2}{4} \chi_1^2 - \frac{\mu_2^2}{4} \chi_2^2 + \frac{1}{2}\Lambda (\Phi^\dagger \Phi) (\chi_1^2 + \chi_2^2) \\ & + \frac{1}{4}\lambda_s (\chi_1^2 + \chi_2^2)^2 + \frac{1}{\sqrt{2}}\kappa_2 (\chi_1^3 - 3\chi_1 \chi_2^2) \\ & + \frac{1}{\sqrt{2}}\kappa_3 (\chi_1^3 + \chi_1 \chi_2^2) + \sqrt{2}\kappa_4 (\Phi^\dagger \Phi) \chi_1. \end{aligned} \quad (9)$$

B. Positivity conditions

In order to have a stable minimum, the parameters of the potential need to satisfy the positivity conditions. The potential should be bounded from below, i.e. should not go to negative infinity for large field values. As this behavior is dominated by the quartic terms, the cubic terms will not play a role here. Thus the following positivity conditions will apply

$$\lambda_1, \lambda_s > 0, \quad \Lambda > -\sqrt{2\lambda_1\lambda_s}. \quad (10)$$

C. Extremum conditions

The extremum conditions lead to the following constraints:

$$-m_{11}^2 + \lambda_1 v^2 + \Lambda w^2 = 0, \quad (11)$$

$$w_1(-\mu_1^2 + v^2\Lambda + 2w^2\lambda_s) + \sqrt{2}[3(w_1^2 - w_2^2)\kappa_2 + (3w_1^2 + w_2^2)\kappa_3] = 0, \quad (12)$$

$$-\mu_2^2 + v^2\Lambda + 2w^2\lambda_s + 2\sqrt{2}w_1(-3\kappa_2 + \kappa_3) = 0, \quad (13)$$

where we use the *vev* for the singlet scalar field in the form: $w e^{i\xi} = w \cos \xi + i w \sin \xi = w_1 + i w_2$ and parameters μ_1^2 and μ_2^2 defined as

$$\mu_1^2 = m_s^2 + 2m_4^2, \quad \mu_2^2 = m_s^2 - 2m_4^2.$$

Various spontaneous symmetry breaking extrema are possible, among them with vanishing one or two of vacuum expectation parameters v, w_1, w_2 . Here we concentrate on the case with v, w_1 and w_2 different from zero, allowing for a vacuum violating CP.

D. The CP violating vacuum

When v and both w_1, w_2 are different from zero an important relation can be obtained by subtracting equation (61) from the equation (60), namely [27]

$$-4m_4^2 \cos \xi + 3R_2(1 + 2 \cos 2\xi) + R_3 = 0, \quad (14)$$

where $R_2 = \sqrt{2}w\kappa_2$ and $R_3 = \sqrt{2}w\kappa_3$, both with $[mass]^2$ dimension.

For a particular case $R_2 = 0$ equation (14) transforms to:

$$\begin{aligned} -4m_4^2 \cos \xi + R_3 &= 0, \quad \cos \xi = \frac{R_3}{4m_4^2} \\ \rightarrow -4m_4^2 < R_3 < 4m_4^2. \end{aligned} \quad (15)$$

The regions of the parameters R_2, R_3 and ξ allowed by Eq. (14), for fixed m_4^2 , are shown in Fig. 1. Figure 2a is a two-dimensional version of the Fig. 1. Another two-dimensional plot showing the allowed regions of R_3 and $4m_4^2$, for R_2 equal zero (Eq. (15)), is presented in Figs. 2b.

III. PHYSICAL STATES IN THE HIGGS SECTOR

Mass squared matrix M_{mix} in the basis of ϕ_1, ϕ_2, ϕ_3 can be written as follows:

$$M_{mix} = \begin{pmatrix} M_{11} & M_{12} & M_{13} \\ M_{21} & M_{22} & M_{23} \\ M_{31} & M_{32} & M_{33} \end{pmatrix}, \quad (16)$$

where the $M_{ij}(i, j = 1, 2, 3)$ are:

$$\begin{aligned} M_{11} &= \frac{1}{2}(-m_{11}^2 + 3v^2\lambda_1 + w^2\Lambda) \\ M_{12} &= vw_1\Lambda \\ M_{13} &= vw_2\Lambda \\ M_{22} &= -m_4^2 - \frac{1}{2}m_s^2 + \frac{1}{2}v^2\Lambda + (w_2^2 + 3w_1^2)\lambda_s \\ &\quad + 3\sqrt{2}w_1(\kappa_2 + \kappa_3) \\ M_{23} &= w_2(2w_1\lambda_s + \sqrt{2}(-3\kappa_2 + \kappa_3)) \\ M_{33} &= m_4^2 - \frac{1}{2}m_s^2 + \frac{1}{2}v^2\Lambda + (w_1^2 + 3w_2^2)\lambda_s \\ &\quad + \sqrt{2}w_1(-3\kappa_2 + \kappa_3). \end{aligned} \quad (17)$$

The extremum condition have not been applied to get M_{ij} elements presented in Eq. (17). When the the extremum condition Eqs. (59-61) is applied the diagonal elements change to

$$\begin{aligned} M_{11} &= v^2\lambda_1, \\ M_{22} &= \frac{w^2}{\sqrt{2}w_1} (3\kappa_2 + \kappa_3(1 + 2(w_1^2 - w_2^2)/w^2)) + 2w_1^2\lambda_s, \\ M_{33} &= 2w_2^2\lambda_s. \end{aligned} \quad (18)$$

Diagonalization of M_{mix}^2 (17) gives the mass-eigenstates h_1, h_2, h_3 :

$$\begin{pmatrix} h_1 \\ h_2 \\ h_3 \end{pmatrix} = R \begin{pmatrix} \phi_1 \\ \phi_2 \\ \phi_3 \end{pmatrix}, \quad R M_{mix}^2 R^T = \text{diag}(M_{h_1}^2, M_{h_2}^2, M_{h_3}^2). \quad (19)$$

We will consider the following mass hierarchy $M_{h_1} < M_{h_2} \lesssim M_{h_3}$.

The rotation matrix $R = R_1 R_2 R_3$ depends on three mixing angles $(\alpha_1, \alpha_2, \alpha_3)$. The individual rotation matrices are given by (here and below $c_i = \cos \alpha_i, s_i = \sin \alpha_i$):

$$\begin{aligned} R_1 &= \begin{pmatrix} c_1 & s_1 & 0 \\ -s_1 & c_1 & 0 \\ 0 & 0 & 1 \end{pmatrix}, \quad R_2 = \begin{pmatrix} c_2 & 0 & s_2 \\ 0 & 1 & 0 \\ -s_2 & 0 & c_2 \end{pmatrix}, \\ R_3 &= \begin{pmatrix} 1 & 0 & 0 \\ 0 & c_3 & s_3 \\ 0 & -s_3 & c_3 \end{pmatrix}. \end{aligned} \quad (20)$$

All α_i vary over an interval of length π . The full rotation matrix R depends on the mixing angles in the following

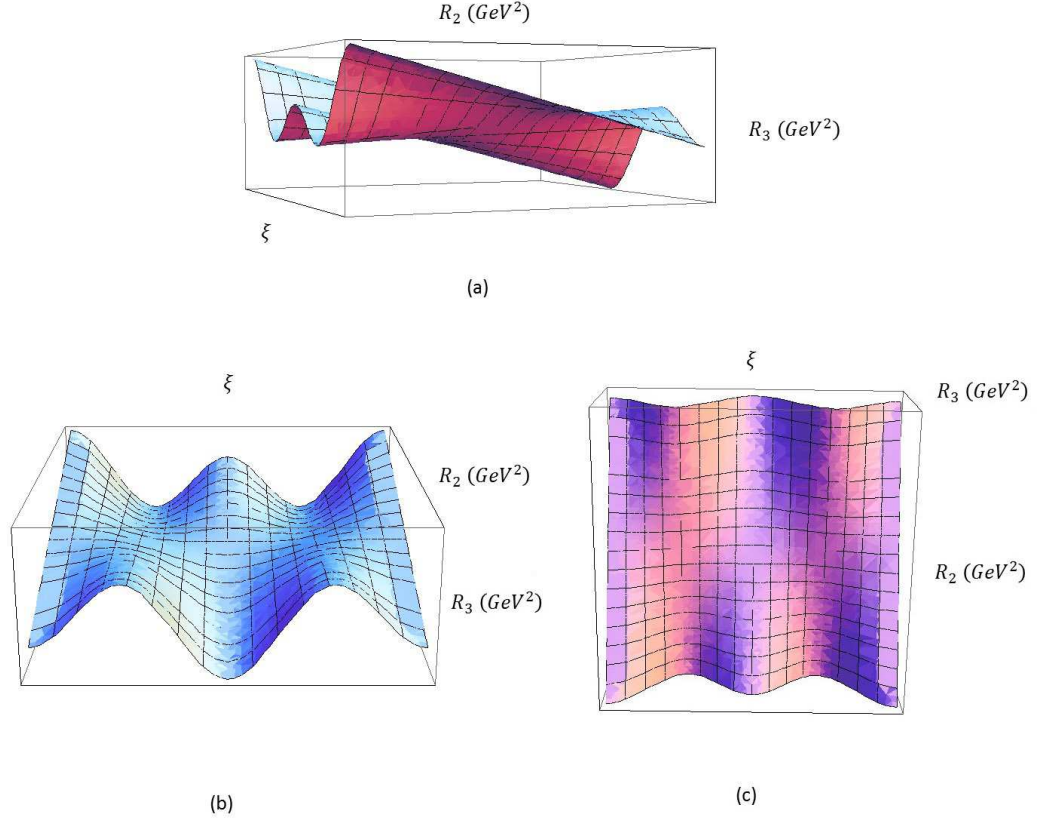


Figure 1. The regions of the parameters R_2 , R_3 and ξ as follows from Eq. (14), for fixed m_4^2 , from different perspectives.

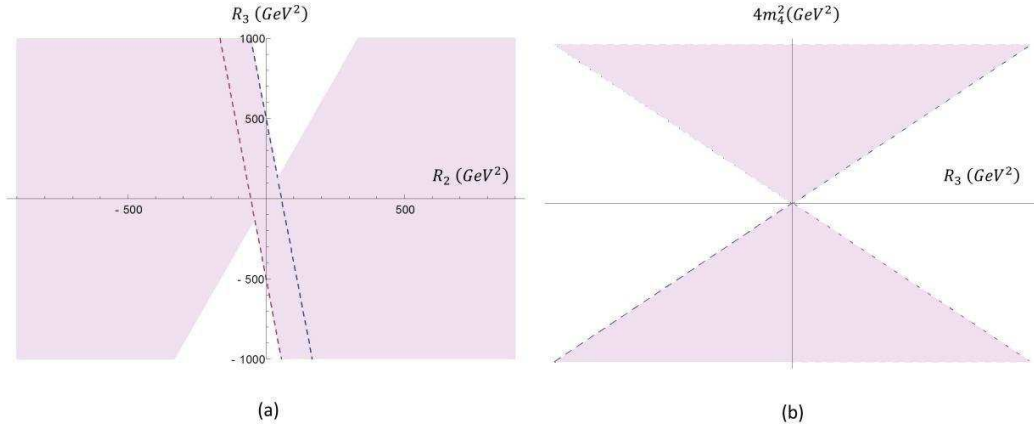


Figure 2. The correlation between the parameters R_2 , R_3 and m_4^2 , for $-1 < \cos \xi < 1$. The dashed lines corresponds to the $\cos \xi = \pm 1$ limits, not allowed for CP violation. (a) Shaded regions for R_2 and R_3 allowed by Eq. (14), at $4m_4^2 = 500$ GeV²; (b) Shaded regions for $4m_4^2$ and R_3 allowed by Eq. (15), for $R_2 = 0$.

manner:

$$R = R_1 R_2 R_3 = \begin{pmatrix} c_1 c_2 & c_3 s_1 - c_1 s_2 s_3 & c_1 c_3 s_2 + s_1 s_3 \\ -c_2 s_1 & c_1 c_3 + s_1 s_2 s_3 & -c_3 s_1 s_2 + c_1 s_3 \\ -s_2 & -c_2 s_3 & c_2 c_3 \end{pmatrix}. \quad (21)$$

The inverse of R can be used to obtain the reverse relation between h_i and ϕ_i .

The element (11) of both rotation matrices R and R^{-1} are equal to

$$R_{(11)} = R_{(11)}^{-1} = c_1 c_2.$$

Two important relations can be read from the above rotation matrices, namely:

$$h_1 = c_1 c_2 \phi_1 + (c_3 s_1 - c_1 s_2 s_3) \phi_2 + (c_1 c_3 s_2 + s_1 s_3) \phi_3 \quad (22)$$

and

$$\phi_1 = c_1 c_2 h_1 - c_2 s_1 h_2 - s_2 h_3. \quad (23)$$

These relations describe the composition of the SM-like Higgs boson h_1 in terms of the CP-even (ϕ_1 and ϕ_2) and the CP-odd (ϕ_3) components. It signals the CP mixing in the model. In the Sec. IV we use these equations to perform a scanning of the relevant regions of parameters. We shall treat h_1 as the 125 GeV Higgs boson.

IV. ALLOWED REGIONS OF PARAMETERS FOR CP VIOLATING VACUUM

In what follows, we present results of a numerical analysis of the allowed regions of parameters of the cSMCS model, with the CP violating vacuum, in agreement with the positivity and extremum conditions as well as the perturbativity conditions. We assume v being bounded to the region $246 \text{ GeV} < v < 247 \text{ GeV}$ and that the mass of the lightest Higgs particle h_1 lies in range

$$M_{h_1} \in [124.00, 127.00] \text{ GeV}, \quad (24)$$

in agreement with recent LHC results for the Higgs boson [30]. We take masses of two additional, heavier Higgs scalars to be [26]

$$M_{h_3} \gtrsim M_{h_2} > 150 \text{ GeV}. \quad (25)$$

The parameters of the Higgs sector are varied in the following ranges:

$$-1 < \Lambda < 1, \quad 0 < \lambda_s < 1, \quad -1 < \rho_{2,3} < 1, \quad 0 < \xi < \pi, \quad (26)$$

where we used dimensionless parameters $\rho_{2,3} = \kappa_{2,3}/w$.

From assumption that $M_{h_1}^2 \approx m_{11}^2 \approx \lambda_1 v^2$, and $M_{h_1} \approx 125 \text{ GeV}$ we estimate range of λ_1 to be :

$$0.2 < \lambda_1 < 0.3. \quad (27)$$

In order to have an appropriate range for the parameter v we set the ranges of remaining quadratic variables as follows:

$$-90000 \text{ GeV}^2 < \mu_1^2, \mu_2^2, m_{11}^2 < 90000 \text{ GeV}^2. \quad (28)$$

The range of values of v_{ev} for the singlet, w , was not set in the analysis - it was derived from the scan. The obtained allowed regions for quartic parameters and masses are shown in Fig. 3. In Fig.3a, the allowed region of Λ versus λ_s is shown. We got strong constraints on the singlet self coupling λ_s , to be greater than 0.2, and on the doublet-singlet coupling $|\Lambda|$, to be below 0.2. Note, that the constraints of Λ and λ_s arise mainly from the

mass limits (24). The positivity condition can constrain only the region of negative Λ , as follows from (10). This is shown as a light shadowed region in the plot Fig.3a. Figs. 3b and 3c show the allowed regions of masses for h_2 and h_3 , respectively. For higher λ_s larger masses are possible, respectively up to 650 and 800 GeV. Note, that larger values of quadratic parameters $|\mu_1^2|, |\mu_2^2|$, beyond the range given in (28), would lead to larger allowed masses for scalars h_2, h_3 .

The allowed regions for the cubic parameters ρ_2 and ρ_3 are important from point of view of CP violation (14), they are shown in Fig. 4. Fig. 4a shows the allowed by scan over parameters the (R_2, R_3) region. Note, that it reproduces roughly results presented on Fig.2a, obtained solely from the extremum conditions (14). In Figs. 4b,c the allowed regions of the phase ξ versus ρ_2, ρ_3 are presented. In both panels there are two allowed regions, symmetric with respect to $\xi \sim \pi/2$, with a gap around the central value $\xi = \pi/2$ (which corresponds to $w_1 \approx 0$).

The result of the scanning over other potential parameters are shown in Fig. 5. In the figure 5a the allowed region of the (w, v) plane is presented. The v_{ev} of singlet w reaches the highest value of 800 GeV, however the most points are concentrated at low value of w (2 - 50 GeV). This is related to the fact that we limit $\lambda_1 \approx m_{11}^2/v^2$ (27), what leads to the small w according to the equation (59). Domination of small w is seen also in the Fig.5c, where the allowed region of w as a function of Λ is shown as well as in Fig.5d, where the w as a function of m_{11}^2 is presented. Here, the concentration of points is observed for value of m_{11}^2 , close to the mass square of the SM Higgs boson, as expected. The allowed regions of ξ versus Λ is shown in Fig. 5b, where a symmetry and a gap for $\xi \sim \pi/2$ is seen in the ξ distributions, as discussed above.

The allowed regions of masses of the Higgs bosons h_2 and h_3 are shown in Fig. 6, once more showing the symmetry and the gap in the ξ distribution. The maximal values of masses, around 650 GeV (h_2) and 800 (h_3) GeV, can be reached for ξ around 1 and symmetrically around 2 radians (i.e. for ξ equal 1.5 ± 0.5 radians).

V. J-INVARIANTS

In this section we estimate the amount of CP violation in the considered cSMCS model using the Jarlskog invariant. C. Jarlskog has introduced such quantity originally for the quark sector [22]. It has been shown that the Jarlskog invariants can be used for the scalars to flag the existence of the CP-violation in the models with an extended scalar sector [23–25]. For 2HDM the discussion of these invariants was performed in e.g. [8, 10, 31]. If the Jarlskog quantity J_1 is different from zero then there is a CP violation in the model.

The J_1 can be defined by mixing elements of the squared mass matrix [62] as follows:

$$J_1 = M_{12}M_{13}(M_{22} - M_{33}) + M_{23}(M_{13}^2 - M_{12}^2), \quad (29)$$

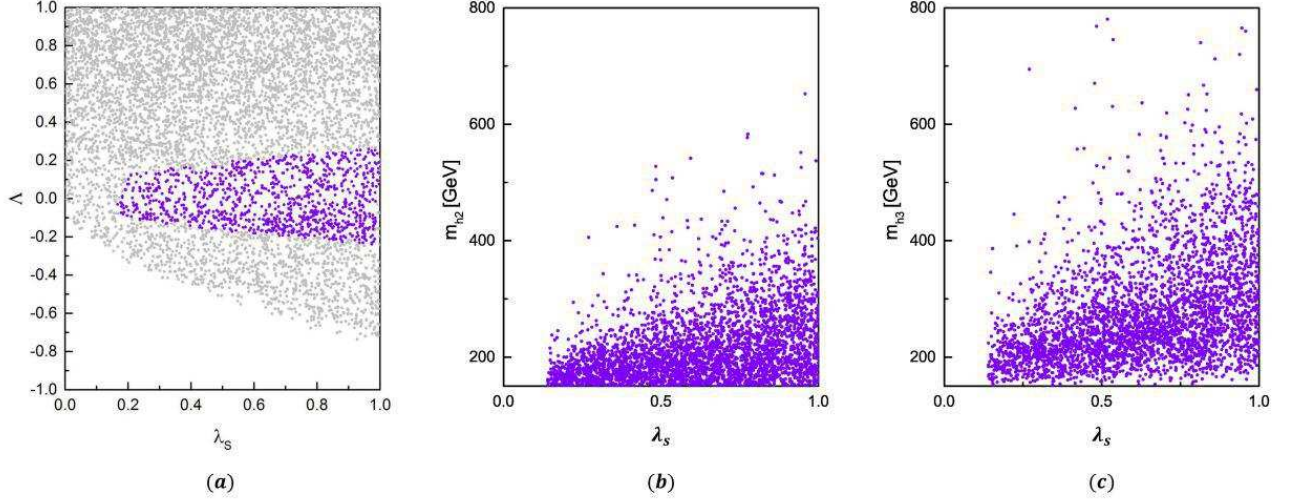


Figure 3. The allowed region for quartic parameters and masses. a) Λ versus λ_s is presented. In the light shaded region only positivity conditions were applied. b) M_{h2} versus λ_s and c) M_{h3} versus λ_s .

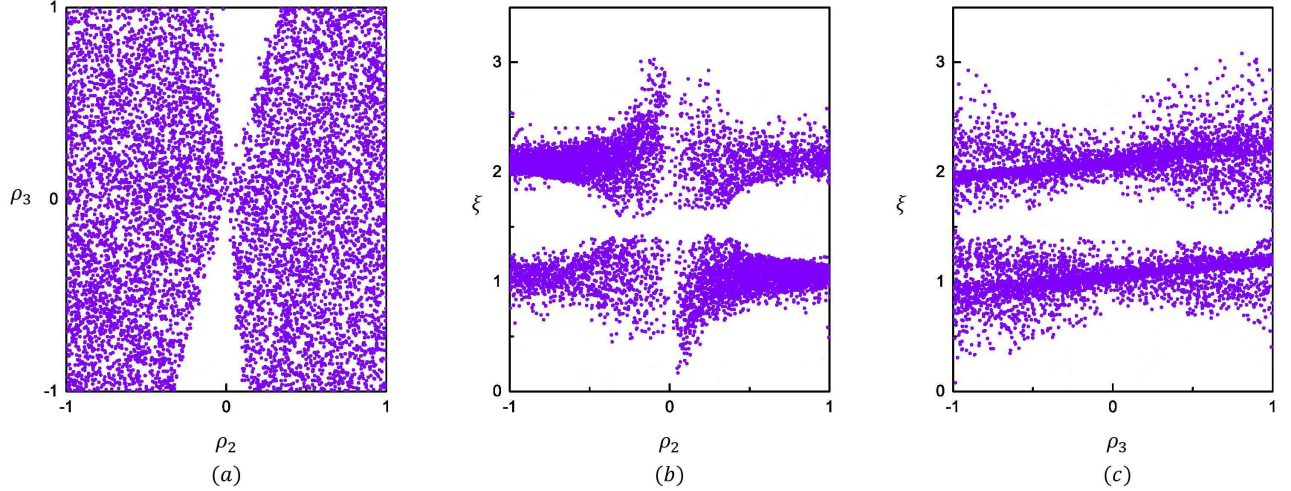


Figure 4. The allowed regions for cubic parameters: a) ρ_2 versus ρ_3 , b) ρ_2 versus ξ , c) ρ_3 versus ξ .

which for vacuum state with CP violation, described by the equation (14), leads to

$$J_1 = 2\Lambda^2 v^2 w^2 m_4^2 \sin \xi \cos \xi = 2\Lambda^2 v^2 w_1 w_2 m_4^2, \quad (30)$$

with m_4^2 given by Eq. (14). So, in order to have $J_1 \neq 0$ the non-vanishing complex vev of a singlet is needed as well as the U(1)-violating quadratic term - m_4^2 . As follows from eq. (14), nonzero value of m_4^2 means non vanishing of at least one cubic term for the singlet. Further - a interaction between a doublet and singlet is necessary. It is well known that in the SM the "true" J_1 invariant is of the order of 10^{-5} [3]. The Fig. 7 shows the range of the dimensionful (GeV^6) invariant J_1 for the considered model. By normalizing it by v^6 , as we choose v to represent temperature of the EW phase transition T_{EW} , we get the highest value for $|J_1/v^6|$ around 10^{-3} . It can be

larger for larger $|m_4^2|$.

In the Appendix IX we calculate the Jarlskog invariant for the case with $\kappa_4 \neq 0$.

VI. COMPARISON WITH DATA

In the considered cSMCS model we examine the SM-like scenario with the lightest neutral Higgs particle being the 125 GeV Higgs particle observed at LHC. Not only mass, but also direct couplings to fundamental particles should be close to the ones measured at the LHC. We found that this is indeed a case for our model. Below we collect main formulas and constraints from the model as coming from the LHC data on 125 GeV Higgs bosons and measurement of oblique corrections. Here we present

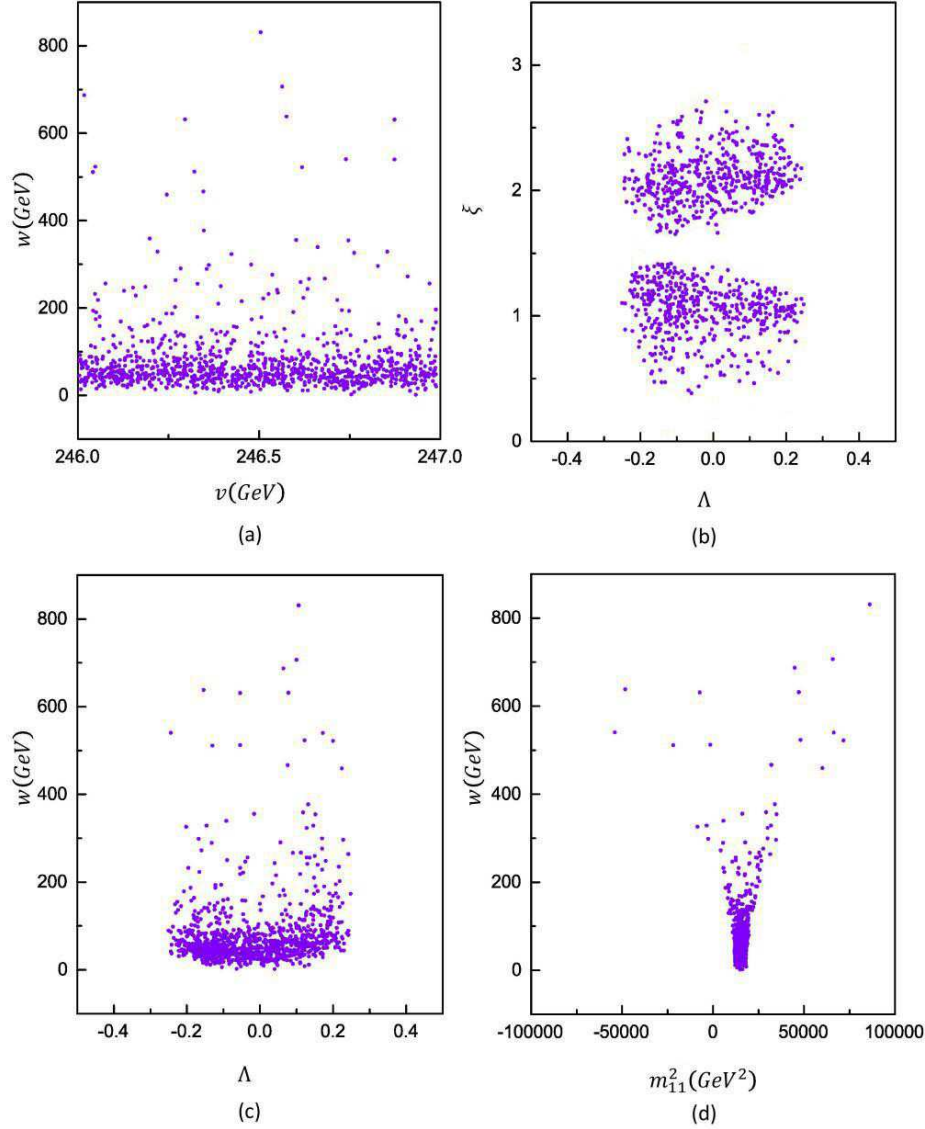


Figure 5. The allowed regions: (a) the correlation between v and w (b) the correlation between Λ and ξ (c) the correlation between w and Λ and (d) w versus m_{11}^2 .

also a short discussion on prediction of the model for the EDM. We finish this section by presenting 7 benchmarks.

A. Properties of h_1 Higgs boson in light of LHC data

The couplings of the lightest Higgs particle (h_1) to the quarks and the gauge bosons in the cSMCS model, as compared with the corresponding couplings of the SM Higgs, are modified (suppressed) by a factor R_{11} (Eq.(21). In particular, for the Higgs boson decay into vector bosons ($V = Z, W$) we have

$$\Gamma(h_1 \rightarrow VV^*) = R_{11}^2 \Gamma(H_{SM} \rightarrow VV^*). \quad (31)$$

Further constraints on the parameters of our model can be obtained by comparing the decay of the light Higgs boson h_1 and of the SM Higgs boson into $\gamma\gamma$. This is done using the signal strength $R_{\gamma\gamma}$:

$$\begin{aligned} \mathcal{R}_{\gamma\gamma} &= \frac{\sigma(gg \rightarrow h_1)}{\sigma(gg \rightarrow H_{SM})} \frac{\text{BR}(h_1 \rightarrow \gamma\gamma)}{\text{BR}(H_{SM} \rightarrow \gamma\gamma)} \\ &= \frac{\Gamma(h_1 \rightarrow gg)}{\Gamma(H_{SM} \rightarrow gg)} \frac{\text{BR}(h_1 \rightarrow \gamma\gamma)}{\text{BR}(H_{SM} \rightarrow \gamma\gamma)}, \end{aligned} \quad (32)$$

taking into account that the production of the Higgs bosons in the LHC is dominated by the gluon fusion processes and that the narrow width approximation can be applied. The Higgs h_1 decay width into gluons is given

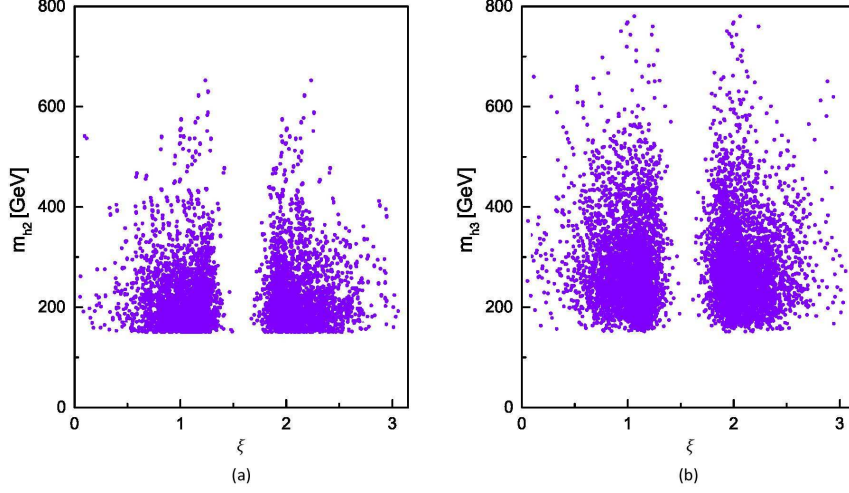


Figure 6. Allowed regions for Higgs masses: a) M_{h_2} versus ξ and b) M_{h_3} versus ξ .

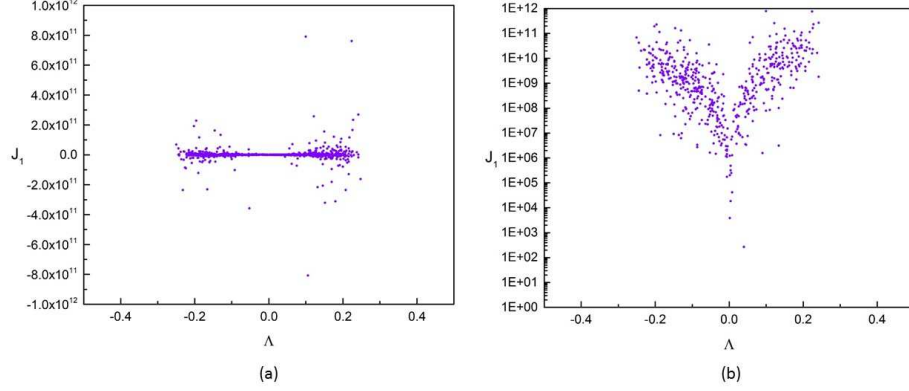


Figure 7. J_1 invariant (in GeV^6) as a function of Λ in linear (a) and log (b) scale.

by:

$$\Gamma(h_1 \rightarrow gg) = R_{11}^2 \Gamma(H_{SM} \rightarrow gg). \quad (33)$$

The main contribution in the one-loop coupling of h_1 to photons is due to the W boson and top quark, and therefore in our model the corresponding amplitude and the decay rate are equal to:

$$\begin{aligned} A(h_1 \rightarrow \gamma\gamma) &= R_{11}(A_W^{SM} + A_t^{SM}) \\ \rightarrow \Gamma(h_1 \rightarrow \gamma\gamma) &= R_{11}^2 \Gamma(H_{SM} \rightarrow \gamma\gamma), \end{aligned} \quad (34)$$

see Appendix (VIII C). Since the total width of the light Higgs boson h_1 is given by

$$\Gamma_{tot} \approx R_{11}^2 \Gamma_{tot}^{SM}, \quad (35)$$

the signal strengths Eq.(32) is equal to

$$\mathcal{R}_{\gamma\gamma} \approx R_{11}^2. \quad (36)$$

Both \mathcal{R}_{VV} and $\mathcal{R}_{\gamma\gamma}$ are smaller than 1, by the same amount, compatible with recent LHC measurements.

Note, that the total decay width for heavier Higgses can be significantly modified with respect to the SM, if h_i (heavier) can decay into the lighter h_j particles, since

$$\Gamma_{tot} \approx R_{i1}^2 \Gamma_{tot}^{SM} + \sum_{i=2,3;j=1,2,3;i>j} \Gamma_{h_i \rightarrow h_j h_j}.$$

The partial decay width for such decay channels $h_i \rightarrow h_j h_j$, where $i > j$, is given by

$$\Gamma(h_i \rightarrow h_j h_j) = \frac{g_{h_i h_j h_j}^2}{32\pi M_{h_i}} \left(1 - \frac{4M_{h_j}^2}{M_{h_i}^2}\right)^{1/2}, \quad (37)$$

where $g_{h_i h_j h_j}$ is the coupling between Higgs bosons, see Appendix (VIII D) for corresponding expressions. In the considered model the signal strength for $\gamma\gamma$ for h_1 as well as for h_2, h_3 can only be smaller than (or equal to) 1. Below, we present our predictions for several benchmarks, all for $R_{11}^2 \sim 0.81 - 0.98$.

B. Oblique parameters S, T, U

The additional particles introduce corrections to the gauge boson propagators in the SM that can be parametrized by the oblique parameters S , T and U . The oblique parameters in cSMCS model, following the method introduced in [33], are described in the Appendix VIII B. Below, we show that chosen by us benchmarks are in agreement with current data for S and T . The values that are determined from a fit with reference mass-values of top and Higgs boson $M_{t,ref} = 173$ GeV and $M_{h,ref} = 125$ GeV read [34]

$$S = 0.05 \pm 0.11, \quad T = 0.09 \pm 0.13, \quad U = 0.01 \pm 0.11. \quad (38)$$

C. EDM

The radiative corrections coming from the contributions of the additional Higgs particles in the Barr-Zee diagrams for EDM [32] turned out to be zero because in our model the scalar singlet does not couple to the SM fermions and pseudoscalar-like Yukawa coupling, that results in the EDM, is absent in our model.

D. Benchmarks

Here we present seven benchmarks for the considered model showing agreement with the above mentioned constraints. Properties of benchmarks are presented in table I and II. Table I shows mixing angle $\alpha_{1,2,3}$ and masses for h_1, h_2 and h_3 . The highest mass of h_3 is 760 GeV while the lowest one is 179 GeV. The table contains as well the prediction of the considered model for the S and T parameters (being in agreement with the current data within 3σ) and J_1/v^6 invariant. The Jarlskog invariant J_1/v^6 can be positive or negative, with range of its (absolute) value from 3.5×10^{-5} to 9.5×10^{-4} .

In table II the calculated $\mathcal{R}_{\gamma\gamma}$ for h_1 as well as h_2 and h_3 are presented together with their total widths. The largest decay widths, from 7 to 17 GeV, are obtained for benchmark A3, A4 and A5 for relatively heavy h_3 (for masses around 600 GeV). Note, that only benchmark points A6 and A7 corresponds to relatively light (mass below 200 GeV) Higgs bosons h_2 and h_3 and only these two benchmarks arise from negative Λ , as presented in Fig. 8.

VII. CONCLUSION AND OUTLOOK

In this paper we present the cSMCS - an extension of the Standard Model containing a complex singlet with a non-zero complex vev , which allows for the spontaneous CP violation. For simplicity, we have performed analysis assuming that doublet-singlet interaction is given by Λ

term only. We have checked that inclusion of κ_4 does not change main properties of the model, allowing for CP violation (Appendix IX) and strong first order phase transition, see also [28].

Within our model different vacua can be realized, here we have focused on the case with the CP violating vacuum. We have derived a simple condition for existence of such vacuum, and found that at least one cubic term for χ is needed in order to have spontaneous CP violation. In the model there are three neutral Higgs particles with indefinite CP properties. The model can easily accommodate the SM-like Higgs, with mass around 125 GeV, in agreement with LHC data and measurements of the oblique parameters. In this respect we confirm basic results obtained for the Higgs sector already in the paper [26], within a larger framework with the additional inert doublet. Note however, that in the present scan we keep w parameter as a free parameter and perform more detailed analysis of allowed parameters of the model and their correlations. In general, this analysis shows that CP violation arises in our model from the scalar interactions between a doublet and a singlet (Λ) and cubic terms κ_2, κ_3 and of course complex vev of the singlet. The calculated Jarlskog invariant J_1 , normalized to v^6 , can reach value 10^{-3} . The singlet-fermion interactions is realized only through mixing of singlet with the doublet and therefore pseudoscalar-like Yukawa coupling is absent in our model, and the prediction for EDM does not exceed the corresponding SM one. We provide seven benchmarks, in agreement with collider data, for future tests of the model.

ACKNOWLEDGEMENTS

We are grateful to G. Branco, M. Rebelo and M. Sampaio for useful discussions. We express our special thanks to Dorota Sokolowska for valuable suggestions and Saereh Najjari for support. The work was partially supported by the grant NCN OPUS 2012/05/B/ST2/03306 (2012-2016) and the National Science Centre, Poland, the HARMONIA project under contract UMO- 2015/18/M/ST2/00518 (2016-2019).

VIII. APPENDIX A

A. Coupling of scalars with gauge bosons and fermions

We can represent rotation of the fields ϕ_i , $i = 1 - 4$

$$\begin{pmatrix} \phi_1 + i\phi_4 \\ \phi_2 + i\phi_3 \end{pmatrix} = P \begin{pmatrix} G^0 \\ h_1 \\ h_2 \\ h_3 \end{pmatrix}, \quad (39)$$

Benchmark	α_1	α_2	α_3	M_{h_1}	M_{h_2}	M_{h_3}	S	T	J_1/v^6
A1	-0.047	-0.053	1.294	124.64	652.375	759.984	-0.072	-0.094	-2.2×10^{-4}
A2	-0.048	0.084	0.084	124.26	512.511	712.407	-0.001	-0.039	7.2×10^{-4}
A3	0.078	0.297	0.364	124.27	582.895	650.531	0.003	-0.046	4.5×10^{-4}
A4	0.006	-0.276	0.188	125.86	466.439	568.059	-0.013	-0.169	-9.5×10^{-4}
A5	0.062	-0.436	0.808	125.21	303.545	582.496	0.002	-0.409	5.0×10^{-6}
A6	-0.210	0.358	0.056	124.92	181.032	188.82	0.003	-0.010	-4.0×10^{-5}
A7	-0.205	0.403	0.057	125.01	175.45	178.52	0.002	-0.020	-3.5×10^{-5}

Table I. Benchmark points A1 – A7, masses are given in GeV.

Benchmark	$R_{\gamma\gamma}^{h_1}$	$R_{\gamma\gamma}^{h_2}$	$R_{\gamma\gamma}^{h_3}$	$\Gamma_{tot}^{h_1}$	$\Gamma_{tot}^{h_2}$	$\Gamma_{tot}^{h_3}$
A1	0.98	0.0021	0.0028	0.0042	0.304	0.781
A2	0.98	0.0021	0.0070	0.0042	0.145	1.31
A3	0.98	0.0055	0.085	0.0042	0.566	12.24
A4	0.92	3.3×10^{-5}	0.074	0.0043	0.001	7.08
A5	0.81	0.0029	0.17	0.0043	0.002	17.51
A6	0.82	0.19	0.11	0.0043	0.119	0.163
A7	0.81	0.18	0.15	0.0043	0.871	0.083

Table II. Values of $R_{\gamma\gamma}$ and Γ_{tot} for benchmark points A1 – A7. The total widths are given in GeV.

where the 2×4 matrix P is equal to

$$P = \begin{pmatrix} i & R_{11} & R_{21} & R_{31} \\ 0 & R_{12} + iR_{13} & R_{22} + iR_{23} & R_{32} + iR_{33} \end{pmatrix}. \quad (40)$$

The kinetic term in \mathcal{L}_{scalar} has the standard form:

$$T_k = (D_\mu \Phi)^\dagger (D^\mu \Phi) + \partial_\chi \partial \chi^*, \quad (41)$$

with D_μ being a covariant derivative for an $SU(2)$ doublet and can be defined as

$$D_\mu = \partial_\mu - igW_\mu^a t^a - ig'Y_\phi B_\mu. \quad (42)$$

The covariant derivative of the neutral singlets is identical with their ordinary derivative:

$$\begin{aligned} T_k &= \frac{1}{2} \partial_\mu h_1 \partial^\mu h_1 + \frac{1}{2} \partial_\mu h_2 \partial^\mu h_2 + \frac{1}{2} \partial_\mu h_3 \partial^\mu h_3 \\ &+ M_w^2 W_\mu^+ W^{-\mu} + \frac{M_z^2}{2} Z_\mu Z^\mu \\ &+ g(M_w W_\mu^+ W^{-\mu} + \frac{M_z^2}{2c_w} Z_\mu Z^\mu) [R_{11}h_1 + R_{21}h_2 + R_{31}h_3] \\ &+ (\frac{g^2}{4} W_\mu^+ W^{-\mu} + \frac{g^2}{8c_w^2} Z_\mu Z^\mu) [R_{11}^2 h_1 h_1 + R_{21}^2 h_2 h_2 \\ &+ R_{31}^2 h_3 h_3 + R_{11}R_{21}h_1 h_2 + R_{11}R_{31}h_1 h_3 + R_{21}R_{31}h_2 h_3] \\ &+ \text{gauge cubic/quartic terms}, \end{aligned} \quad (43)$$

that quadratic terms give masses to the W and Z bosons: $M_W = \frac{1}{2}v|g|$, $M_Z = \frac{1}{2}v\sqrt{g^2 + g'^2}$. Since the neutral singlet field carries no hypercharge, its vev does not contribute to the masses of the gauge bosons. \mathcal{L}_Y contains the *Yukawa* interactions between the fermions and the Higgs fields that generates the fermion masses after the Higgs acquires a vacuum expectation value. Notice that only the doublet couples to the fermions.

$$\mathcal{L}_Y = - \sum_f \frac{m_f}{\nu} \bar{f} f (R_{11}h_1 + R_{21}h_2 + R_{31}h_3) \quad (44)$$

The charged current part of the Lagrangian is given by:

$$\begin{aligned} \mathcal{L}_C &= -\frac{g}{\sqrt{2}} \left[\bar{u}_i \gamma^\mu \frac{1-\gamma^5}{2} M_{ij}^{CKM} d_j + \bar{\nu}_i \gamma^\mu \frac{1-\gamma^5}{2} e_i \right] W_\mu^+ \\ &+ h.c. \end{aligned} \quad (45)$$

B. Oblique parameters

To study the contributions to oblique parameters in the cMSSM, we use the method presented in [33]. S and T parameters in the cMSSM are given by:

$$\begin{aligned} T &= \frac{g^2}{64\pi^2 M_W^2 \alpha_{em}} \left\{ - (R_{12}R_{23} - R_{13}R_{22})^2 F(M_{h_1}^2, M_{h_2}^2) \right. \\ &- (R_{12}R_{33} - R_{13}R_{32})^2 F(M_{h_1}^2, M_{h_3}^2) \\ &- (R_{22}R_{33} - R_{32}R_{22})^2 F(M_{h_2}^2, M_{h_3}^2) \\ &+ 3(R_{11})^2 (F(M_Z^2, M_{h_1}^2) - F(M_W^2, M_{h_1}^2)) \\ &- 3(F(M_Z^2, M_{h_{ref}}^2) - F(M_W^2, M_{h_{ref}}^2)) \\ &+ 3(R_{21})^2 (F(M_Z^2, M_{h_2}^2) - F(M_W^2, M_{h_2}^2)) \\ &\left. + 3(R_{31})^2 (F(M_Z^2, M_{h_3}^2) - F(M_W^2, M_{h_3}^2)) \right\} \end{aligned} \quad (46)$$

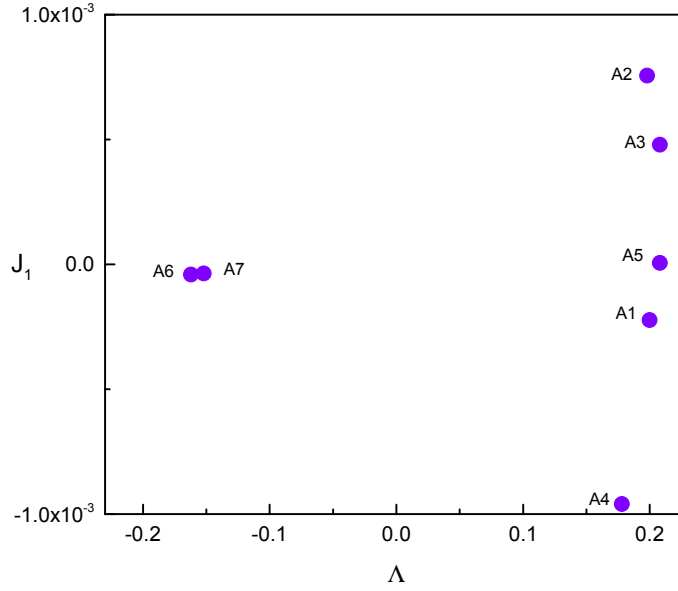


Figure 8. J_1 invariant (divided by v^6) for the benchmarks points.

and

$$S = \frac{g^2}{384\pi^2 C_w^2} \left\{ (R_{12}R_{23} - R_{13}R_{22})^2 G(M_{h_1}^2, M_{h_2}^2, M_Z^2) \right. \\ + (R_{12}R_{13} - R_{13}R_{32})^2 G(M_{h_1}^2, M_{h_3}^2, M_Z^2) \\ + (R_{22}R_{33} - R_{32}R_{22})^2 G(M_{h_2}^2, M_{h_3}^2, M_Z^2) \\ + (R_{11})^2 \hat{G}(M_{h_1}^2, M_Z^2) - \hat{G}(M_{h_{ref}}^2, M_Z^2) \\ + (R_{21})^2 \hat{G}(M_{h_2}^2, M_Z^2) + (R_{31})^2 \hat{G}(M_{h_3}^2, M_Z^2) \\ + \log(M_{h_1})^2 - \log(M_{h_{ref}})^2 + \log(M_{h_2})^2 \\ \left. + \log(M_{h_3})^2 \right\}, \quad (47)$$

where the following functions have been used

$$F(M_1^2, M_2^2) = \frac{1}{2}(M_1^2 + M_2^2) - \frac{M_1^2 M_2^2}{M_1^2 - M_2^2} \log\left(\frac{M_1^2}{M_2^2}\right), \quad (48)$$

$$G(m_1, m_2, m_3) = \frac{-16}{3} + \frac{5(m_1 + m_2)}{m_3} - \frac{2(m_1 - m_2)^2}{m_3^2} \\ + \frac{3}{m_3} \left[\frac{m_1^2 + m_2^2}{m_1 - m_2} - \frac{m_1^2 - m_2^2}{m_3} \right. \\ \left. + \frac{(m_1 - m_2)^3}{3m_3^2} \right] \log \frac{m_1}{m_2} + \frac{r f(t, r)}{m_3^3}, \quad (49)$$

The function f is given by

$$f(t, r) = \begin{cases} \sqrt{r} \ln \left| \frac{t - \sqrt{r}}{t + \sqrt{r}} \right| & r > 0, \\ 0 & r = 0, \\ 2\sqrt{-r} \arctan \frac{\sqrt{-r}}{t} & r < 0, \end{cases} \quad (50)$$

with the arguments defined as

$$t \equiv m_1 + m_2 - m_3, \quad r \equiv m_3^2 - 2m_3(m_1 + m_2) + (m_1 - m_2)^2. \quad (51)$$

Finally, $\hat{G}(m_1, m_2)$ can be written as follows

$$\hat{G}(m_1, m_2) = \frac{-79}{3} + 9\frac{m_1}{m_2} - 2\frac{m_1^2}{m_2^2} + \left(-10 + 18\frac{m_1}{m_2} \right. \\ \left. - 6\frac{m_1^2}{m_2^2} + \frac{m_1^3}{m_2^3} - 9\frac{m_1 + m_2}{m_1 - m_2} \right) \log \frac{m_1}{m_2} \\ + (12 - 4\frac{m_1}{m_2} + \frac{m_1^2}{m_2^2}) \frac{f(m_1, m_1^2 - 4m_1 m_2)}{m_2}. \quad (52)$$

C. Decays $h \rightarrow \gamma\gamma$

The decay width, $\Gamma(h \rightarrow \gamma\gamma)$, is given by [35, 36],

$$\Gamma(h_1 \rightarrow \gamma\gamma) = R_{11}^2 \Gamma(\phi_{SM} \rightarrow \gamma\gamma). \quad (53)$$

Then the ratio $R_{\gamma\gamma}$ turns out,

$$\mathcal{R}_{\gamma\gamma} = R_{11}^2 \quad (54)$$

where the form factors for this decay are

$$A_t^{SM} = \frac{4}{3} A_{1/2} \left(\frac{4M_t^2}{M_{h_1}^2} \right), \quad A_W^{SM} = A_1 \left(\frac{4M_W^2}{M_{h_1}^2} \right), \quad (55)$$

where

$$A_{1/2}(\tau) = 2\tau [1 + (1 - \tau)f(\tau)], \\ A_1(\tau) = -[2 + 3\tau + 3\tau(2 - \tau)f(\tau)], \\ A_0(\tau) = -\tau [1 - \tau f(\tau)], \quad (56)$$

and

$$f(\tau) = \begin{cases} \arcsin^2(1/\sqrt{\tau}) & \text{for } \tau \geq 1 \\ -\frac{1}{4} \left(\log \frac{1 + \sqrt{1 - \tau}}{1 - \sqrt{1 - \tau}} - i\pi \right)^2 & \text{for } \tau < 1 \end{cases} \quad (57)$$

D. Higgs trilinear couplings

For coupling among Higgs bosons we have

$$g_{h_2 h_1 h_1} = \frac{1}{2} \left[R_{13}^2 (\Lambda R_{21} v + R_{22} (-3\sqrt{2}\kappa_2 + \sqrt{2}\kappa_3 + 2\lambda_s w_1) + 6\lambda_s R_{23} w_2) + R_{12}^2 (\Lambda R_{21} v + 3R_{22} (\sqrt{2}(\kappa_2 + \kappa_3) + 2\lambda_s w_1) + 2\lambda_s R_{23} w_2) + R_{11}^2 (3\lambda_1 R_{21} v + \Lambda (R_{23} w_2 + R_{22} w_1)) + 2\Lambda R_{11} (R_{13} (R_{23} v + R_{21} w_2) + R_{12} (R_{22} v + R_{21} w_1)) + 2R_{12} R_{13} (R_{23} (-3\sqrt{2}\kappa_2 + \sqrt{2}\kappa_3 + 2\lambda_s w_1) + 2\lambda_s R_{22} w_2) \right]. \quad (58)$$

The $g_{h_3 h_1 h_1}$ coupling can be obtained from the above expression by substitution $R_{2j} \rightarrow R_{3j}$, and for $g_{h_3 h_2 h_2}$ by substitution $R_{2j} \rightarrow R_{3j}$ and then $R_{1j} \rightarrow R_{2j}$.

IX. APPENDIX B: A CASE OF $\kappa_4 \neq 0$

Here we consider the case with $\kappa_4 \neq 0$.

A. The extremum conditions

The extremum conditions lead to the following constraints,

$$-m_{11}^2 + v^2 \lambda_1 + w^2 \Lambda + 2\sqrt{2} w_1 \kappa_4 = 0, \quad (59)$$

$$w_1 (-\mu_1^2 + v^2 \Lambda + 2w^2 \lambda_s) + \sqrt{2} [3(w_1^2 - w_2^2) \kappa_2 + (3w_1^2 + w_2^2) \kappa_3] + v^2 \sqrt{2} \kappa_4 = 0, \quad (60)$$

$$-\mu_2^2 + v^2 \Lambda + 2w^2 \lambda_s + 2\sqrt{2} w_1 (-3\kappa_2 + \kappa_3) = 0. \quad (61)$$

B. Physical states in the Higgs sector

Mass squared matrix M_{mix} in the basis of ϕ_1, ϕ_2, ϕ_3 can be written as follows:

$$M_{mix} = \begin{pmatrix} M_{11} & M_{12} & M_{13} \\ M_{21} & M_{22} & M_{23} \\ M_{31} & M_{32} & M_{33} \end{pmatrix}, \quad (62)$$

where the $M_{ij} (i, j = 1, 2, 3)$ are:

$$\begin{aligned} M_{11} &= v^2 \lambda_1, \\ M_{12} &= v(w_1 \Lambda + \sqrt{2} \kappa_4), \\ M_{13} &= v w_2 \Lambda, \\ M_{22} &= \frac{w^2}{\sqrt{2} w_1} (3\kappa_2 + \kappa_3 (1 + 2(w_1^2 - w_2^2)/w^2) - \kappa_4 v^2/w^2) + 2w_1^2 \lambda_s, \\ M_{23} &= w_2 (2w_1 \lambda_s + \sqrt{2} (-3\kappa_2 + \kappa_3)), \\ M_{33} &= 2w_2^2 \lambda_s. \end{aligned} \quad (63)$$

The equation for CP violating vacuum is modified as compared to the condition (14) as follows

$$-4m_4^2 \cos \xi + 3R_2 (1 + 2 \cos 2\xi) + R_3 + R_4 = 0, \quad (64)$$

where

$$R_2 = \sqrt{2} w \kappa_2, \quad R_3 = \sqrt{2} w \kappa_3, \quad R_4 = \frac{\sqrt{2} v^2 \kappa_4}{w},$$

all of which are of $[mass]^2$ dimension. In addition we have

$$R_4 = \frac{v^2}{2w^2 \cos \xi} (m_{11}^2 - v^2 \lambda_1 - w^2 \Lambda).$$

C. J-invariant

The J_1 can be defined by mixing elements of the squared mass matrix [62] and is equal to

$$\begin{aligned} J_1 &= v^2 w_2 \times \\ &\left[w^2 \Lambda^2 (1/\sqrt{2}) (\kappa_3 + 3\kappa_2 (1 + 2(w_1^2 - w_2^2)/w^2) - \kappa_4 v^2/w^2) \right. \\ &\quad - \kappa_4 \Lambda (w^2/w_1) (\sqrt{2} \lambda_s w_1 + \kappa_3 - 3\kappa_2 (3 + 2(w_1^2 - w_2^2)/w^2) \\ &\quad + \kappa_4 v^2/w^2) \\ &\quad \left. + 4\kappa_4^2 (\lambda_s w_1 + (\kappa_3 - 3\kappa_2)/\sqrt{2}) \right]. \end{aligned} \quad (65)$$

Note, that even for $\Lambda = \kappa_2 = \kappa_3 = 0$ the J_1 is not vanishing: $J_1 = 4v^2 w_2 w_1 \kappa_4^2 \lambda_s$.

[1] A. D. Sakharov, Pisma Zh. Eksp. Teor. Fiz. **5** (1967) 32 [JETP Lett. **5** (1967) 24] [Sov. Phys. Usp. **34** (1991) 392]

[Usp. Fiz. Nauk **161** (1991) 61].

- [2] For reviews, see: A. G. Cohen, D. B. Kaplan and A. E. Nelson, *Ann. Rev. Nucl. Part. Sci.* **43**, 27 (1993) [hep-ph/9302210]; M. Quiros, *Helv. Phys. Acta* **67**, 451 (1994); V. A. Rubakov and M. E. Shaposhnikov, *Usp. Fiz. Nauk* **166**, 493 (1996) [*Phys. Usp.* **39**, 461 (1996)] [hep-ph/9603208]; M. S. Carena and C. E. M. Wagner [hep-ph/9704347]; M. Quiros, hep-ph/9901312.
- [3] W. Bernreuther, *Lect. Notes Phys.* **591** (2002) 237 [hep-ph/0205279].
- [4] M. B. Gavela, M. Lozano, J. Orloff and O. Pene, *Nucl. Phys. B* **430** (1994) 345 [hep-ph/9406288].
- [5] M. B. Gavela, P. Hernandez, J. Orloff, O. Pene and C. Quimbay, *Nucl. Phys. B* **430** (1994) 382 [hep-ph/9406289].
- [6] D. Comelli, M. Pietroni and A. Riotto, *Nucl. Phys. B* **412** (1994) 441 [hep-ph/9304267].
- [7] E. Accomando *et al.*, hep-ph/0608079.
- [8] H. E. Haber and Z. Surujon, *Phys. Rev. D* **86** (2012) 075007 [arXiv:1201.1730 [hep-ph]].
- [9] I. F. Ginzburg and M. Krawczyk, *Phys. Rev. D* **72** (2005) 115013 doi:10.1103/PhysRevD.72.115013 [hep-ph/0408011].
- [10] J. F. Gunion and H. E. Haber, *Phys. Rev. D* **72** (2005) 095002 [hep-ph/0506227].
- [11] S. Davidson, R. González Felipe, H. Serôdio and J. P. Silva, *JHEP* **1311** (2013) 100 doi:10.1007/JHEP11(2013)100 [arXiv:1307.6218 [hep-ph]].
- [12] S. Profumo, M. J. Ramsey-Musolf and G. Shaughnessy, *JHEP* **0708** (2007) 010 [arXiv:0705.2425 [hep-ph]].
- [13] G. C. Branco, P. A. Parada and M. N. Rebelo, hep-ph/0307119. L. Bento, G. C. Branco and P. A. Parada, *Phys. Lett. B* **267** (1991) 95.
- [14] E. Gabrielli, M. Heikinheimo, K. Kannike, A. Racioppi, M. Raidal and C. Spethmann, *Phys. Rev. D* **89** (2014) 1, 015017 doi:10.1103/PhysRevD.89.015017 [arXiv:1309.6632 [hep-ph]].
- [15] J. Kozaczk, *JHEP* **1510** (2015) 135 doi:10.1007/JHEP10(2015)135 [arXiv:1506.04741 [hep-ph]].
- [16] M. Jiang, L. Bian, W. Huang and J. Shu, *Phys. Rev. D* **93**, no. 6, 065032 (2016) doi:10.1103/PhysRevD.93.065032 [arXiv:1502.07574 [hep-ph]].
- [17] L. Alexander-Nunneley and A. Pilaftsis, *JHEP* **1009** (2010) 021 doi:10.1007/JHEP09(2010)021 [arXiv:1006.5916 [hep-ph]].
- [18] V. Barger, P. Langacker, M. McCaskey, M. Ramsey-Musolf and G. Shaughnessy, *Phys. Rev. D* **79** (2009) 015018 doi:10.1103/PhysRevD.79.015018 [arXiv:0811.0393 [hep-ph]].
- [19] J. R. Espinosa, B. Gripaios, T. Konstandin and F. Riva, *JCAP* **1201** (2012) 012 [arXiv:1110.2876 [hep-ph]].
- [20] R. Costa, A. P. Morais, M. O. P. Sampaio and R. Santos, *Phys. Rev. D* **92** (2015) 025024 [arXiv:1411.4048 [hep-ph]].
- [21] O. Lebedev, *Phys. Lett. B* **697** (2011) 58 [arXiv:1011.2630 [hep-ph]].
- [22] C. Jarlskog, *Phys. Rev. Lett.* **55**, 1039 (1985)
- [23] L. Lavoura, *Phys. Rev. D* **50** (1994) 7089 doi:10.1103/PhysRevD.50.7089 [hep-ph/9405307].
- [24] L. Lavoura and J. P. Silva, *Phys. Rev. D* **50** (1994) 4619 [hep-ph/9404276].
- [25] F. J. Botella and J. P. Silva, *Phys. Rev. D* **51** (1995) 3870 [hep-ph/9411288].
- [26] C. Bonilla, D. Sokolowska, N. Darvishi, J. L. Diaz-Cruz and M. Krawczyk, arXiv:1412.8730 [hep-ph].
- [27] M. Krawczyk, N. Darvishi and D. Sokolowska, *Acta Phys. Polon. B* **47** (2016) 183 doi:10.5506/APhysPolB.47.183 [arXiv:1512.06437 [hep-ph]].
- [28] N. Darvishi, arXiv:1608.02820 [hep-ph].
- [29] M. Sampaio - private communication
- [30] S. Chatrchyan *et al.* [CMS Collaboration], *Phys. Lett. B* **716** (2012) 30 [arXiv:1207.7235 [hep-ex]]. G. Aad *et al.* [ATLAS Collaboration], *Phys. Lett. B* **716** (2012) 1 [arXiv:1207.7214 [hep-ex]].
- [31] D. Sokolowska, K. A. Kanishev and M. Krawczyk, *PoS CHARGED* **2008** (2008) 016 [arXiv:0812.0296 [hep-ph]].
- [32] S. M. Barr and A. Zee, *Phys. Rev. Lett.* **65**, 21 (1990) [Erratum-ibid. **65**, 2920 (1990)].
- [33] W. Grimus, L. Lavoura, O. M. Ogreid and P. Osland, *Nucl. Phys. B* **801** (2008) 81 [arXiv:0802.4353 [hep-ph]].
- [34] M. Baak *et al.* [Gfitter Group Collaboration], *Eur. Phys. J. C* **74** (2014) 9, 3046 [arXiv:1407.3792 [hep-ph]].
- [35] B. Swiezewska and M. Krawczyk, *Phys. Rev. D* **88** (2013) 3, 035019 [arXiv:1212.4100 [hep-ph]].
- [36] A. Djouadi, *Phys. Rept.* **459**, 1 (2008) [hep-ph/0503173].